Expression of a RecQ Helicase Homolog Affects Progression through Crisis in Fission Yeast Lacking Telomerase*

Jeffrey G. Mandell‡§, Karen J. Goodrich‡, Jürg Bähler¶, and Thomas R. Cech‡||

From the ‡Department of Chemistry and Biochemistry and Howard Hughes Medical Institute, University of Colorado, Boulder, Colorado 80309-0215 and ¶The Wellcome Trust Sanger Institute, Cambridge CB10 1SA, United Kingdom

RecQ helicases play roles in telomere maintenance in cancerous human cells using the alternative lengthening of telomeres mechanism and in budding yeast lacking telomerase. Fission yeast lacking the catalytic subunit of telomerase ($trt1^+$) up-regulate the expression of a previously uncharacterized sub-telomeric open reading frame as survivors emerge from crisis. Here we show that this open reading frame encodes a protein with homology to RecQ helicases such as the human Bloom's and Werner's syndrome proteins and that copies of the helicase gene are present on multiple chromosome ends. Characterization of the helicase transcript revealed a 7.6-kilobase RNA that was associated with polyribosomes, suggesting it is translated. A 3.6-kilobase domain of the helicase gene predicted to encode the region with catalytic activity was cloned, and both native and mutant forms of this domain were overexpressed in $trt1^-$ cells as they progressed through crisis. Overexpression of the native form caused cells to recover from crisis earlier than cells with a vector-only control, whereas overexpression of the mutant form caused delayed recovery from crisis. Taken together, the sequence homology, functional analysis, and site-directed mutagenesis indicate that the protein is likely a second fission yeast RecQ helicase (in addition to Rqh1) that participates in telomere metabolism during crisis. These results strengthen the notion that in multiple organisms RecQ helicases contribute to survival after telomere damage.

The RecQ family of helicases is conserved from prokaryotes to humans and contributes to such critical functions as genomic stability and repair of stalled replication forks (1, 2). Mutations in three of the five human RecQ helicases, BLM,[1] WRN, and RECQ4, cause Bloom's syndrome, Werner's syndrome, and Rothmund-Thomson syndrome, respectively (for review, see Ref. 1). Symptoms include premature aging of the skin, vasculature, and bone in Werner's syndrome and short stature and limited premature aging in Bloom's syndrome. All three disorders are associated with an increased predisposition to cancer. Unicellular organisms such as yeast typically express a single RecQ homolog, such as Sgs1 in budding yeast and Rqh1 in fission yeast.

RecQ proteins share a helicase domain with seven highly conserved motifs (I, Ia, II-VI) (3). Regions that vary both in size and in sequence may flank the helicase domain, but little sequence similarity exists beyond these motifs (4). All characterized RecQ helicases can unwind DNA in an ATP-dependent manner in the 3′ to 5′ direction in relation to the DNA strand to which the enzyme is bound. WRN and BLM cannot bind to and unwind blunt-ended B-form DNA but require a single-stranded binding site, such as a 3′ overhang, to initiate unwinding of duplex DNA (5). Furthermore, RecQ helicases are apparently unique among helicases in their ability to unwind different forms of G-quadruplexes (5, 6) that may form at telomeres (7–9). Additionally, WRN can resolve intramolecular D loops that likely form at telomeres (10, 11).

Telomeres are the nucleoprotein ends of linear eukaryotic chromosomes. Telomeric DNA generally consists of a simple, repeated sequence with a G-rich strand running 5′ to 3′ toward the chromosome end, and it terminates with a single-stranded 3′ overhang (for review, see Refs. 12 and 13). In most eukaryotes, this telomeric DNA is synthesized by the enzyme telomerase, a reverse transcriptase consisting of an RNA subunit, a catalytic protein (encoded by $trt1^+$ in *Schizosaccharomyces pombe*), and additional protein subunits (14). Telomerase adds sequence complementary to its internal RNA template to chromosome ends. In the absence of telomerase cells lose telomeric DNA and eventually senesce when cell division ceases. However, rare cells can emerge from senescence and continue to divide indefinitely using alternate telomere maintenance mechanisms. Telomerase-independent telomere maintenance occurs in cancerous human ALT cells and in both budding and fission yeast lacking telomerase (15–18).

Interestingly, WRN and BLM associate with telomeric DNA exclusively in ALT cells (11, 19), and both WRN and BLM associate with duplex telomere repeat-binding protein TRF2 (20) *in vivo* (11, 19, 21, 22). Furthermore, overexpression of the BLM helicase leads to rapid, ALT cell-specific increases in telomeric DNA synthesis (19). The budding yeast RecQ helicase Sgs1 functions in the Rad50/Rad52 recombination pathway for telomerase-independent telomere maintenance and is required for telomere elongation of type II survivors (23–25). These findings strongly support a role for RecQ helicases in telomerase-independent telomere maintenance. Likewise, the observation that Werner's syndrome cells, which do not normally express telomerase, display accelerated telomere erosion and premature senescence (26) that can be rescued by expression of the telomerase catalytic subunit (27) also suggests that RecQ helicases have important functions at telomeres.

[1] The abbreviations used are: BLM, Bloom's syndrome protein; WRN, Werner's syndrome protein; ALT, alternative lengthening of telomeres; ORF, open reading frame; RACE, rapid amplification of cDNA ends; YES, yeast extract full supplements; contig, group of overlapping clones; HRDC, helicase RNase D C-terminal; RQC, RecQ family C-terminal; kb, kilobase(s).

In a study to investigate telomerase-independent survival of fission yeast, we analyzed global expression profiles of strains lacking $trt1^+$ (28). A previously uncharacterized ORF annotated as a putative helicase had virtually no expression in wild-type cells but had substantially increased expression in survivors emerging from crisis. Strikingly, it was the only gene identified to have altered expression at such a late time in the recovery from loss of telomerase. This putative helicase has sequenced copies (SPAC212.11 and SPBCPT2R1.08c) on two sub-telomeres and in one case is only ~10 kb from the telomeric repeats (28). On the basis of a homology search we hypothesized that these genes encode a new member of the RecQ helicase family and contribute to fission yeast telomerase-independent telomere maintenance.

Here we show that this putative helicase has significant homology to RecQ helicases and that copies of the helicase reside on all four sub-telomeres of chromosomes I and II. Furthermore, cells overexpressing a domain of this helicase exit from crisis sooner than controls, whereas cells overexpressing a catalytically inactive form of the helicase have a delayed exit from crisis.

EXPERIMENTAL PROCEDURES

Gene Annotations—Sequences and other annotations were taken from *S. pombe* GeneDB (www.genedb.org/genedb/pombe/index.jsp) and the *S. pombe* Genome Project (www.sanger.ac.uk/Projects/S_pombe). Unless otherwise stated, helicase amino acid and base numbering refer to the annotated record for SPAC212.11.

Differences between the Two Helicase Copies in Data Base—The data base (GeneDB) contains two copies of a sub-telomeric ORF annotated as a putative helicase, SPAC212.11 (5.6 kb) and SPBCPT2R1.08c (6.3 kb), residing on the left arm of chromosome I and the right arm of chromosome II, respectively. The annotated sequence of SPBCPT2R1.08c includes the entirety of SPAC212.11 with one silent base substitution, resulting in identical predicted protein sequences over the entire length of SPAC212.11. The size difference between the two ORFs (~700 bp) reflects additional 5′ and 3′ sequence in SPBCPT2R1.08c, well outside of the predicted helicase domain. The extra 5′ sequence is due to a predicted start codon that is located 543 bp upstream with respect to the predicted SPAC212.11 start codon. The SPAC212.11 sequence has five base changes or deletions in this 5′ region that introduce stop codons. The additional 3′ sequence in SPBCPT2R1.08c results from a premature end to the SPAC212 sequencing contig, resulting in the lack of a stop codon for SPAC212.11. Comparison with the SPBCPT2R1.08c sequence suggests SPAC212.11 has an additional 95 bp before its stop codon.

Because the data base entries for these two ORFs are essentially identical throughout the predicted helicase domain and flanking regions, references to the SPAC212.11 ORF are equally applicable to the SPBCPT2R1.08c ORF. It is not known whether one or both of these ORFs are transcribed, although results presented here indicate the existence of only a single transcript species.

RACE, Gene Cloning, and Site-directed Mutagenesis—Whole cell RNA (1 μg) prepared as described (28) from strain H1 (see "Plasmids and Strains," this section) was used to create a 5′ RACE (rapid amplification of cDNA ends)-ready cDNA library using the SMART RACE cDNA amplification kit (BD Biosciences) following the manufacturer's protocol. 5′ RACE was performed using the gene-specific primer 5′-GTACTGGTAGTCCTCTGATGTATGGG-3′ and the SMART II A oligonucleotide, and 3′ RACE was performed with the gene-specific primer 5′-ATGCCCCGTACGCTTATCTA-3′ and oligo-dT$_{18}$. Gene-specific primers were chosen on the basis of their proximity to the annotated ends of SPAC212.11. Ten clones were chosen from each RACE reaction and sequenced to establish a consensus.

Using primers derived from 5′ and 3′ RACE sequencing results, end-to-end PCR was performed with the 5′ primer 5′-AACGACACCG-GACAGTCGGGAACAACGTTTGC-3′ and the 3′ primer 5′-CATTGAT-GCATATTTCAGCTTTATTTTCATTTCATTCG-3′ (named helicase-end). The helicase domain (from the codon specifying methionine 804 in SPAC212.11 to the end of the cDNA as determined by 3′ RACE) was amplified by PCR from the RACE cDNA library using gene-specific primers 5′-ATGTCTAAGAAGGATCTGACAAAGTTGTTTGGTGG-3′ (named helicase-start) and helicase-end (see above), with a BamHI site on the 5′ end of helicase-start and a SacI site on the 5′ end of helicase-

end (endonuclease sequences not shown). The resulting 3.6-kb fragment (henceforth referred to as the "native" form of the helicase) was cloned into the BamHI and SacI sites of vector pBluescript KS+ (Stratagene, La Jolla, CA) and sequenced to confirm the absence of mutations. All helicase-cloning steps were performed using GeneHogs *Escherichia coli* cells (Invitrogen).

The double mutation K1219M::D1322N was introduced to render the helicase catalytically inactive. Mutations were performed sequentially using the QuikChange II site-directed mutagenesis kit (Stratagene) according to the manufacturer's instructions and were confirmed by sequencing.

To assess protein expression levels, a FLAG tag with amino acid sequence DYKDDDDK (31) was inserted using PCR just after the start codon in both the native and mutant forms of the helicase. The resulting PCR fragment with BamHI and SacI ends was subcloned into expression vector pART1-KanMX6 (described below in "Plasmids and Strains," this section).

Plasmids and Strains—Plasmid pART1 (32) was chosen as a base plasmid because of its constitutive fission yeast alcohol dehydrogenase (adh) promoter (33). The LEU2 marker of pART1 is flanked by HindIII sites and was removed by digestion, resulting in plasmid pART1-LEU2. The 1460-bp KanMX6 cassette (34) was amplified by PCR from plasmid pKan1 (35) using primers designed to incorporate AatII ends and to disrupt the terminal SacI cloning site with the base change T to A. The resulting PCR fragment was cloned into the single AatII site of pART1-LEU2, creating plasmid pART1-KanMX6. The directionality of the KanMX6 cassette was not determined. FLAG-helicase fusion fragments with 5′-BamHI and 3′-SacI ends (described above) were cloned into the unique BamHI and SacI sites of pART1-KanMX6.

The three plasmids used in this study were pART1-KanMX6 ("vector-only") and pART1-KanMX6 with either the native or mutant helicase sequence following the adh (alcohol dehydrogenase) promoter. Plasmids were transformed into either diploid strain G4 (h^-/h^+ ade6-M210/ade6-M216 $trt1^+/trt1^-$) (28) or wild-type strain WT-5 (h^- ade6-M210) (28) using the lithium acetate method (36). After transformation cells were grown in the presence of Geneticin disulfate (Sigma) at 100 μg/ml to maintain selective pressure for plasmids. Single colonies resulting from transformations were chosen and propagated. As described previously (28), diploid strains were germinated to generate haploid cells that were subsequently screened for the genotype (h^- ade6-M210) and the presence or absence of $trt1^+$ and used in growth curves (described below in "Growth Curves," this section). Growth curves with wild-type cells (Fig. 5) were performed with transformants from strain WT-5, whereas growth curves in Figs. 6 and 7 were carried out with transformants derived from strain G4.

Strain H1 is a $trt1^-$ isolate with circular chromosomes, as evidenced by pulsed-field gel electrophoresis (data not shown) and its gene expression profile (28). Strain H1 constitutively expresses abundant helicase transcript as determined by microarray (data not shown), reverse transcription-PCR (data not shown), and Northern blotting (Fig. 3C).

Alignments—Amino acid alignment was performed with ClustalW Version 1.81 (37) using the Blosum30 weight matrix, a gap open penalty of 10, and a gap extension penalty of 0.05.

Polysome Profiles—Polysome profiles were performed with extract from strains WT 5 ($trt1^+$) and H1 ($trt1^-$) (28) essentially as described (38). Cells were grown to a density of ~4.5 × 10^6 cells/ml in yeast extract full supplements (YES) medium (39), and cycloheximide (Sigma) was added (100 μg/ml) 5 min before harvest. Cells (~10 × 10^8) were washed twice in LHB buffer (10 mM Tris-HCl, pH 7.5, 100 mM NaCl, 30 mM MgCl$_2$, and 100 μg/ml cycloheximide) (38) and lysed using 425–600-μm glass beads (Sigma) and two 30-s bursts at full speed in a FastPrep Instrument (Qbiogene, Carlsbad, CA). Extract (200 μl) containing ~60 A_{260} absorbance units was fractionated through a 7–47% sucrose gradient as described (38). Fractions were treated with proteinase K (0.2 mg/ml) at 37 °C for 30 min, and RNA was extracted with acidic phenol:chloroform (Sigma) followed by chloroform and then ethanol-precipitated. The 80 S subunit was identified by comparison with a polysome profile performed in the presence of 15 mM EDTA to partially dissociate the 80 S subunit.

Northern Hybridizations—RNA was quantified by A_{260}, and samples were subjected to denaturing formaldehyde gel electrophoresis on a 1% agarose gel as described (40). After transfer of RNA to a positively charged nylon membrane (Hybond-N+ membrane, Amersham Biosciences) by capillary transfer and immobilization by UV cross-linking (40), regions of the membrane containing molecular weight markers (RNA ladder (New England Biolabs) and/or 10 μg of total *S. pombe* RNA for the ribosomal RNA bands) were cut off and stained with methylene blue (0.04%).

Probes for $act1^+$, $P_{5'}$ and $P_{3'}$ (sequences described in Ref. 28) were generated by PCR amplification from a genomic DNA template and were gel-purified. Probes were labeled by random-primed transcription of PCR products with the use of [α-^{32}P]dCTP and High Prime Mix (Roche Applied Science). Hybridizations were carried out in Church-Gilbert buffer at 50 °C (41) with $\sim 1 \times 10^7$ cpm of probe. The membrane was washed in 0.1% SDS and 0.1% SSC ($1\times$ SSC = 0.15 M NaCl and 0.015 M sodium citrate) after hybridization and imaged using a PhosphorImager (Amersham Biosciences). For subsequent re-probing of the blot, hybridized probe was removed by washing the membrane 3×10 min in stripping buffer (40 mM Tris-HCl, pH 7.5, 0.1% SDS, 0.1× SSC) at 80 °C and exposing the membrane overnight to confirm removal of signal.

Immunoblotting—Single colonies from transformed wild-type strain WT-5 were grown at 32 °C in 12 ml of YES medium with Geneticin to a density of $\sim 2 \times 10^7$ cells/ml. Protein was prepared as described previously (35), except that cells were lysed using three 30-s bursts at full speed in a FastPrep Instrument. Total protein concentration was determined by Bradford Assay (Pierce), and ~ 50 μg of protein per lane was loaded onto a 4–20% Tris-glycine Novex gel (Invitrogen). Protein was transferred to a ZetaBind positively charged nylon membrane (PerkinElmer Life Sciences). The membrane was first probed with anti-FLAG M2 monoclonal antibody (Sigma) used at a 1:1000 dilution followed by goat anti-mouse antibody (horseradish peroxidase-conjugated) (Chemicon, Temecula, CA) used at a 1:4000 dilution. Protein bands were visualized with the ECL chemiluminescence kit (Amersham Biosciences).

Growth Curves—Growth curves were performed essentially as described (28). Briefly, single colonies were used to inoculate 5-ml starter cultures in YES medium (with Geneticin at 100 μg/ml when appropriate) and grown for 24 h with shaking at 32 °C. Cells were counted and used to inoculate YES cultures (either 100 ml in 500-ml Erlenmeyer flasks or 10 ml in 50-ml tubes) at 5.0×10^4 cells/ml. At the end of every 24-h period, cells were counted and used to inoculate fresh cultures at 5.0×10^4 cells/ml, and the process was repeated for 15 days. A portion of cells from 100-ml cultures was set aside for analysis by Southern blotting. Where noted, biological repeats ($n = 2$) were treated identically but were started from separate single colonies. When the repeats were similar, the data points were averaged and are displayed with *error bars* that span the range of averaged values.

RESULTS

Homology with RecQ Helicases—The data base (GeneDB) contains two copies of the putative helicase genes (SPAC212.11 and SPBCPT2R1.08c) with nearly identical helicase coding DNA sequences (see "Experimental Procedures" for differences between the two ORFs). A BLAST search performed with the predicted protein sequence of SPAC212.11 indicated that the most significant homology is with RecQ DNA helicases of Superfamily II (BLAST Expect value = 5×10^{-112}) (for review, see Ref. 1). This homology was significant for residues ~ 1180 to ~ 1820 (including the RecQ and associated RecQ family C-terminal (RQC) and helicase RNase D C-terminal (HRDC) domains; see below). SPAC212.11 was also classified with other RecQ helicases in the NCBI Clusters of Orthologous Groups (COG) data base (42). Note that significant homologies ($E \sim 1 \times 10^{-25}$) to other helicase families were also found, preventing an unequivocal assignment to a particular family.

A subset of relevant human and yeast RecQ orthologs was chosen, and the protein sequences were aligned with SPAC212.11. In all cases, the alignment was highly significant ($E \le 7 \times 10^{-18}$) (Fig. 1A). A schematic alignment of the orthologs on the basis of their RecQ helicase domains also indicated similar sizes for RecQ-related motifs (Fig. 1A).

A protein sequence alignment of SPAC212.11 with selected RecQ orthologs showed significant similarity within the seven helicase consensus motifs (Fig. 1B), including the putative ATP binding site (motif I or the Walker A-box motif) and the DEXH box (motif II or the Walker B-box motif) (3, 43). The obvious similarity of SPAC212.11 with the other proteins is mainly confined to the conserved RecQ helicase domain. The RQC domain (box A in Fig. 1A), thought to mediate protein-protein interactions, has low homology among the various RecQ helicases and can be absent from some family members or have enough sequence divergence to make identification difficult (1). The HRDC domain (box B in Fig. 1A) is believed to be involved in DNA interactions (1).

A phylogenetic analysis showed that all five helicases are evolutionarily approximately equidistant, but that SPAC212.11 is most closely related in sequence to human WRN (44) (Fig. 1C). We, therefore, conclude that SPAC212.11 and SPBCPT2R1.08c are most likely members of the RecQ helicase family, although functional analysis is required for positive identification.

Helicase Duplicated on Multiple Chromosome Ends—The sub-telomeric regions of chromosomes I and II have significant similarity (45). To determine whether regions of homology to SPAC212.11 and SPBCPT2R1.08c exist at other chromosome ends in wild-type cells, we performed pulsed-field gel electrophoresis of NotI-digested chromosomes followed by Southern hybridization with probe $P_{5'}$ (Fig. 1A) specific for the sub-telomeric helicase. SPAC212.11 and SPBCPT2R1.08c reside on the left arm of chromosome I and the right arm of chromosome II, respectively (The *S. pombe* Genome Project). However, hybridization signals were observed for the terminal C, I, L, and M fragments of chromosomes I and II, suggesting that the helicase is present on at least four chromosome ends (Fig. 2, A and B). It is possible that only two complete helicase copies are currently in the data base (GeneDB) because the sub-telomeric sequences from Chromosomes I and II are incomplete.[2]

Full-length Helicase Transcript—The annotations for SPAC212.11 and SPBCPT2R1.08c list predicted transcript lengths of 5.6 and 6.3 kb, respectively. Furthermore, the annotation for SPAC212.11 had no stop codon. RACE was, therefore, used to investigate the actual length of the transcript(s). Transcript ends were identified from ~ 800 bases of consensus sequence derived from ten 5' clones and ~ 600 bases of consensus sequence ascertained from ten 3' clones (data not shown). These sequence data were mapped onto sub-telomeric contig SPBCPT2R1 (The *S. pombe* Genome Project), which spans the range of sequence data obtained by RACE. Using the RACE data, a transcript size of 7603 bases was predicted with no identified introns. This predicted sequence was deposited into GenBank™.

To verify the existence of a 7.6-kb helicase transcript in the RACE cDNA pool, end-to-end PCR was performed using primers specific for the helicase cDNA termini, and a single ~ 7.6-kb PCR product was obtained (data not shown). The presence of a single PCR product could mean that the genes for SPAC212.11 and SPBCPT2R1.08c both yield identical transcripts or, alternatively, that only one of the two genes is transcribed. These possibilities require further investigation given the differences between these genes 5' of their start codons. As described below, the full-length PCR product could not be cloned for sequencing, but a 3.6-kb portion was sequenced and found to be consistent with the predicted 7603-base sequence.

The 7603-base transcript includes ~ 1060 bases and ~ 1600 bases 5' of the annotated start codons of SPBCPT2R1.08c and SPAC212.11, respectively. Furthermore, there are an additional 241 bases 3' of the stop codon in SPBCPT2R1.08c. Although the annotated sequence for SPAC212.11 did not include a stop codon, the sequence experimentally obtained by RACE confirmed an additional 95 bases from the annotated SPAC212.11 end until the stop codon, consistent with the SPBCPT2R1.08c annotation.

Transcript Associated with Polyribosomes—To examine whether the helicase RNA was translated, we determined its

---

[2] R. Hyppa and G. Smith, personal communication.
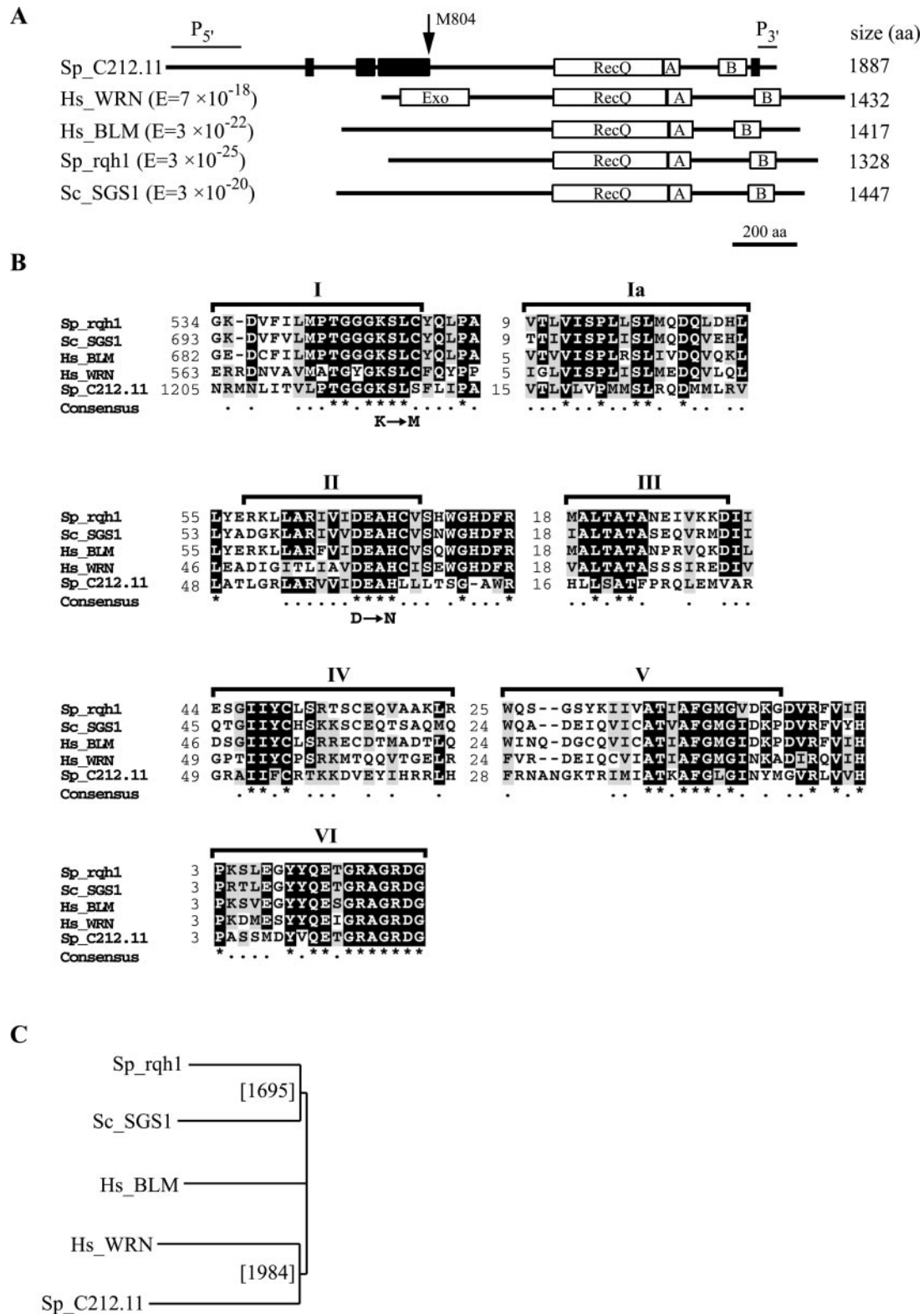
FIG. 1. **Homology of SPAC212.11 with RecQ helicases.** *A*, schematic representations of RecQ helicases. *Sp_C212.11* is *S. pombe* SPAC212.11, *Hs_WRN* is *Homo sapiens* Werner's syndrome protein (44), *Hs_BLM* is *H. sapiens* Bloom's syndrome protein (58), *Sp_rqh1* is *S. pombe* RecQ helicase Rqh1 (59), and *Sc_SGS1* is *S. cerevisiae* RecQ helicase Sgs1p (60). Sequences are aligned based on their conserved helicase domains (RecQ). BLAST E values report homology with SPAC212.11. Boxes labeled *A* and *B* are the conserved RQC and HRDC domains, respectively, and are putatively defined for SPAC212.11. The *vertical arrow* marks methionine 804, the N-terminal boundary of the helicase domain cloned herein. Protein sequences corresponding to nucleic acid probes $P_{5'}$ and $P_{3'}$ used for hybridization are delineated. *Solid black rectangles* are regions of homology with *dh* repeats (28). The box labeled *Exo* is the WRN exonuclease domain. *B*, multiple sequence alignment of the RecQ helicase domains of proteins described in *A*. *Brackets above* the *alignment* mark the seven helicase domains (3). The number of amino acids from the beginning of the polypeptide or between blocks is indicated. *Black-shaded residues* are identical in four or more sequences, and *light-gray shaded residues* are similar in four or more sequences. Identical columns of residues have the consensus symbol *, whereas similar columns have the symbol ●. The two residues mutated in this study are indicated. *C*, a possible phylogenetic tree created using the Neighbor Joining method (61) and bootstrapped 2000 times using residues 804–1887 of SPAC212.11 and the complete sequences of WRN, BLM, SGS1, and Rqh1. *Numbers* in *brackets* indicate the number of times the bootstrapping method gave each branch of the tree.

A
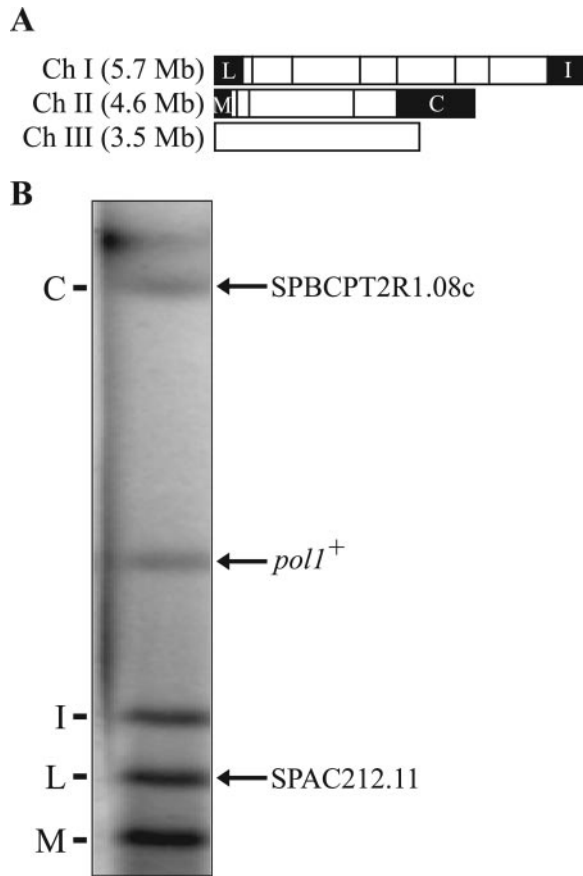
FIG. 2. **The helicase gene resides on multiple chromosome ends.** *A*, the 13 NotI restriction sites in *S. pombe* chromosomes I and II are indicated by *vertical lines* (62). Terminal fragments are labeled according to convention and are *highlighted* in *black*. *B*, pulsed-field gel of NotI-digested chromosomes from wild-type strain WT 3 (28). The gel was transferred to a nylon membrane and probed with ^{32}P-labeled fragment P$_{5'}$ (Fig. 1*A*) and as a loading control, a labeled fragment of the single copy gene *pol1*[+] that resides on fragment F near the middle of chromosome I (62). The terminal fragments of chromosomes I and II are labeled on the *left* and were identified by comparison with size markers on the ethidium bromide-stained gel (not shown). SPAC212.11 resides on terminal fragment L, and SPBCPT2R1.08c is located on fragment C (The *S. pombe* Genome Project). The band at the top of the gel is of unknown origin. Preparation of DNA and electrophoresis were performed as described previously (39).

association with polyribosomes. Crude cell lysates both from *trt1*^{+} cells and from *trt1*^{−} cells expressing an easily detectable amount of helicase transcript (strain H1, see "Experimental Procedures") were fractionated by sucrose gradient centrifugation (Fig. 3*A*). RNA was purified from pooled fractions and used to perform Northern hybridizations with probes to the actin mRNA (*act1*[+]) and to the 3′ end of the helicase transcript (probe P$_{3'}$, Fig. 1*A*).

Active polyribosomes were identified by their location in the sucrose gradient and by their association with the *act1*[+] transcript (Fig. 3*B*). Using probe P$_{3'}$, a single ~7.5-kb transcript was detected in *trt1*^{−} cells; it comigrated with active polyribosomes (Fig. 3*C*). The size of this transcript was consistent with that determined by RACE and end-to-end PCR (7.6 kb). After stripping and rehybridizing the blots with probe P$_{5'}$ (Fig. 1*A*) to the 5′ end of the helicase mRNA, a single transcript of the same size (data not shown) was observed for *trt1*^{−} cells, thus confirming the identity of the observed transcript. The helicase mRNA could not be detected by Northern hybridization in whole-cell RNA from *trt1*^{+} cells, consistent with it not being expressed in wild-type strains (28).
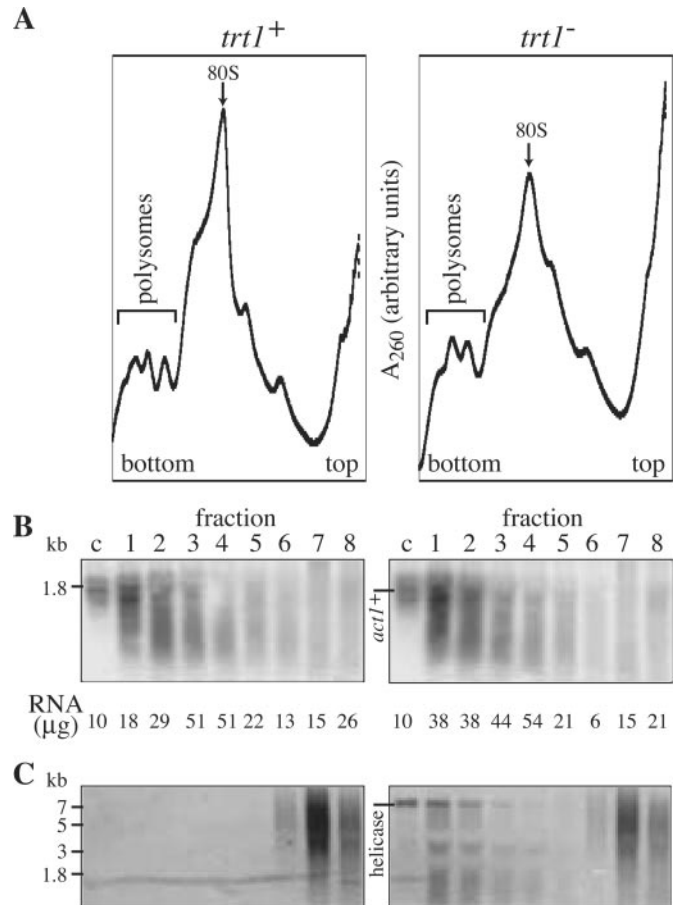
FIG. 3. **Association of the helicase transcript with polyribosomes.** *A*, polysome profiles. Whole-cell RNA from either *trt1*[+] or *trt1*^{−} cells was fractionated on a sucrose gradient, which was removed from the bottom while monitored by A_{260}. The location of the 80 S ribosomal subunit is marked. *B*, Northern blots of RNA collected in *A* probed with a ^{32}P-labeled fragment of *act1*[+]. Collected RNA was pooled into eight fractions; each fraction is aligned with the region of the A_{260} trace from which it came. The amount of RNA (µg) in each fraction is shown *below* the *blots*. The second largest of the three expected *act1*[+] transcripts (30) is marked on the *trt1*[−] blot (and is also seen on the *trt1*[+] blot). Fractions *c* are unfractionated whole-cell RNA from either *trt1*[+] or *trt1*[−] strains that was purified over a Qiagen RNeasy column removing DNA. *C*, as in *B*, using probe P$_{3'}$. The helicase transcript is marked on the *trt1*[−] blot but was not detectable on the *trt1*[+] blot. The hybridization signal apparent in fractions 7 and 8 (*C*) is believed to arise from sheared genomic DNA. This signal is not seen in *B* because only the lower molecular weight region is shown. Treatment of the blot with DNase I eliminated the hybridization signal in fractions from the top of the gradient, whereas treatment with RNase A did not degrade the signal (data not shown).

Cloning the Helicase Gene—To facilitate functional studies, we chose to clone a subdomain of the 7.6-kb helicase cDNA since the 5′ end of the ORF became deleted when full-length PCR products of the cDNA were propagated in *E. coli*. This deletion was likely promoted by a region of *dh* repeats (46) present in the helicase gene (Fig. 1*A*) (28), and deletion persisted even in a recombination-deficient *rec*A1 mutant *E. coli* strain (data not shown). A 3.6-kb subdomain was, therefore, cloned that spanned from the codon specifying methionine (Met-804, Fig. 1*A*) to the end of the cDNA as determined by RACE (thus, 241 bp beyond the stop codon). Met-804 was chosen as the N terminus because it is ~400 amino acids N-terminal to the beginning of the seven canonical helicase domains (3); this large amount of sequence was expected to retain any substrate-specific binding domains. A mutant helicase was also made with two amino acid changes, expected to abolish catalytic activity (Fig. 1*B*). One mutation was in the

A

B
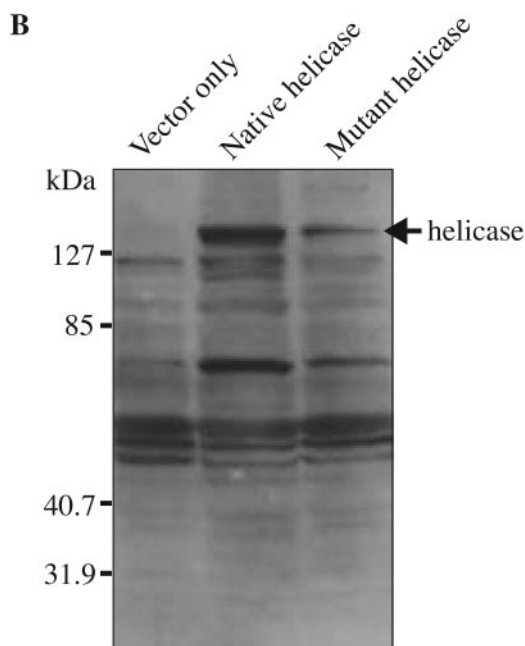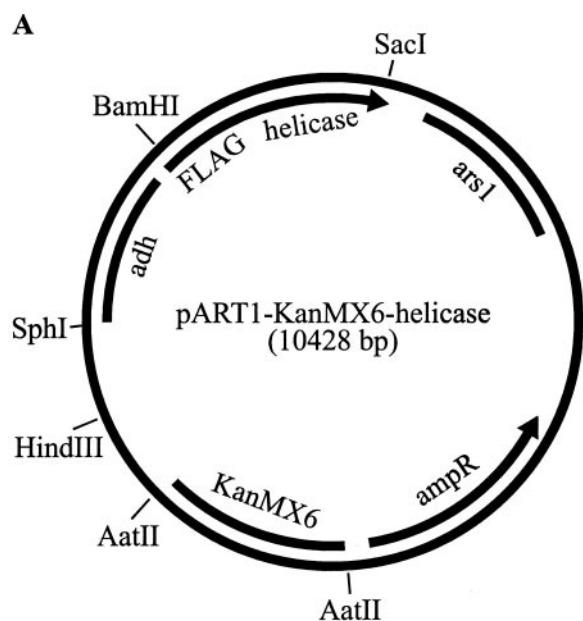
FIG. 4. **Overexpression of the helicase.** *A*, the overexpression plasmid had the FLAG-helicase gene inserted into the BamHI and SacI sites of pART1-KanMX6. The vector-only construct (pART1-KanMX6) had no sequence between the BamHI and SacI sites. *KanMX6*, the gene conferring resistance to Geneticin (34); *adh*, the constitutive fission yeast alcohol dehydrogenase promoter (33); *ars1*, the autonomous replication sequence (29); *ampR*, β-lactamase gene. Gaps between labeled segments are not drawn to scale. *B*, protein extract was prepared from representative wild-type strains transformed with vector only or vector with either the native or mutant helicase sequence. The immunoblot was probed with an anti-FLAG antibody (31), detailed under "Experimental Procedures." Full-length protein has an expected size of 128,531 Da.

Walker A GKS nucleotide binding motif (Lys to Met), and the other was in the Walker B DEAH nucleotide binding/hydrolysis domain (Asp to Asn) (43, 47, 48).

Both the native and mutant forms of the helicase domain were cloned into vector pART1-KanMX6, which confers resistance to the drug Geneticin (Fig. 4*A*). This vector contains the constitutive fission yeast alcohol dehydrogenase promoter (33) permitting high levels of protein expression (49). An inducible
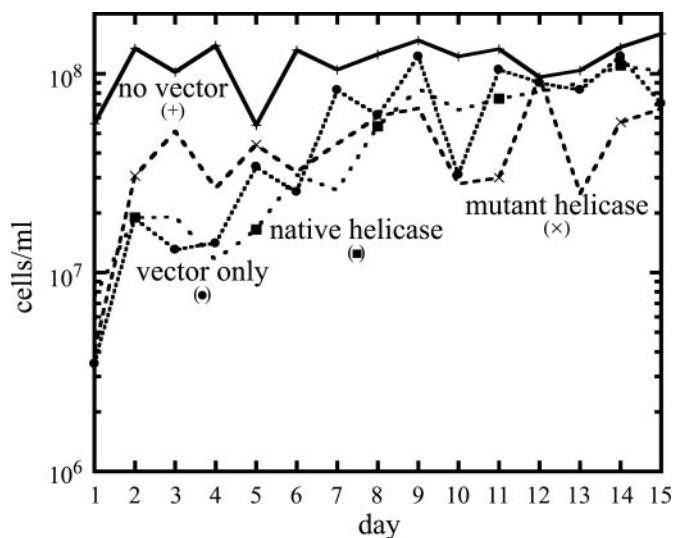
FIG. 5. **Growth curves for helicase overexpression in wild-type cells.** Single colonies were used to inoculate 10-ml cultures that were counted and diluted every 24 h for 15 days (see "Experimental Procedures"). Cell density is shown for cells with no vector (*solid line*, +) and cells transformed with either vector only (*broken line*, ●), vector with the native helicase sequence (*broken line*, ■), or vector with the mutant helicase sequence (*broken line*, ×). All cultures except *No vector* were grown in the presence of Geneticin.

promoter such as $nmt1^+$ (50) was not chosen to avoid putting sickly $trt1^-$ cells through crisis in minimal media.

Helicase Overexpression in Wild-type Cells—Wild-type cells were transformed with vector only or with vector containing the native or mutant helicase sequences. Protein expression was assessed by performing an immunoblot with an antibody directed against the helicase N-terminal FLAG tag (31). Compared with the vector-only control, a clearly detectable band the size of full-length protein (~128.5 kDa) was present on the gel for both lanes with extract from strains overexpressing the helicase. An additional band at ~70 kDa in both lanes suggested a degradation intermediate (Fig. 4*B*). Northern blotting also indicated an abundance of full-length transcript with no substantial degradation products (data not shown). Hybridization signals to overexpressed helicase transcript were at least 10-fold greater than the constitutive level of transcript from SPAC212.11/SPBCPT2R1.08c in $trt1^-$ strain H1 (data not shown).

To test for toxicity resulting from plasmid pART1-KanMX6 or from the overexpressed native or mutant helicase, a 15-day growth curve was performed for wild-type cells bearing different forms of the plasmid (Fig. 5). The three cultures containing Geneticin had lower growth rates than the culture with no drug for days early in the growth curve, but their densities approached that of the no-drug culture on later days. The density increase with time suggested that cells became acclimated to growth in Geneticin. A similar increase in cell density with time was expected to occur with $trt1^-$ cells grown in the presence of Geneticin. Because the vector-only strain behaved similarly to the strains overexpressing helicase protein, there was no obvious toxicity resulting from the overexpressed protein. However, $trt1^+/trt1^-$ heterozygous diploids (strain G4, see "Experimental Procedures") overexpressing the mutant helicase formed ragged colonies, suggesting a toxicity in these cells from the mutant helicase (data not shown).

Testing Function of Helicase in $trt1^-$ Cells—We next investigated the effect of overexpressing the native form of the helicase in $trt1^-$ cells progressing through crisis. Overexpression of the native helicase was potentially expected to amplify the effects of protein expressed from the wild-type helicase
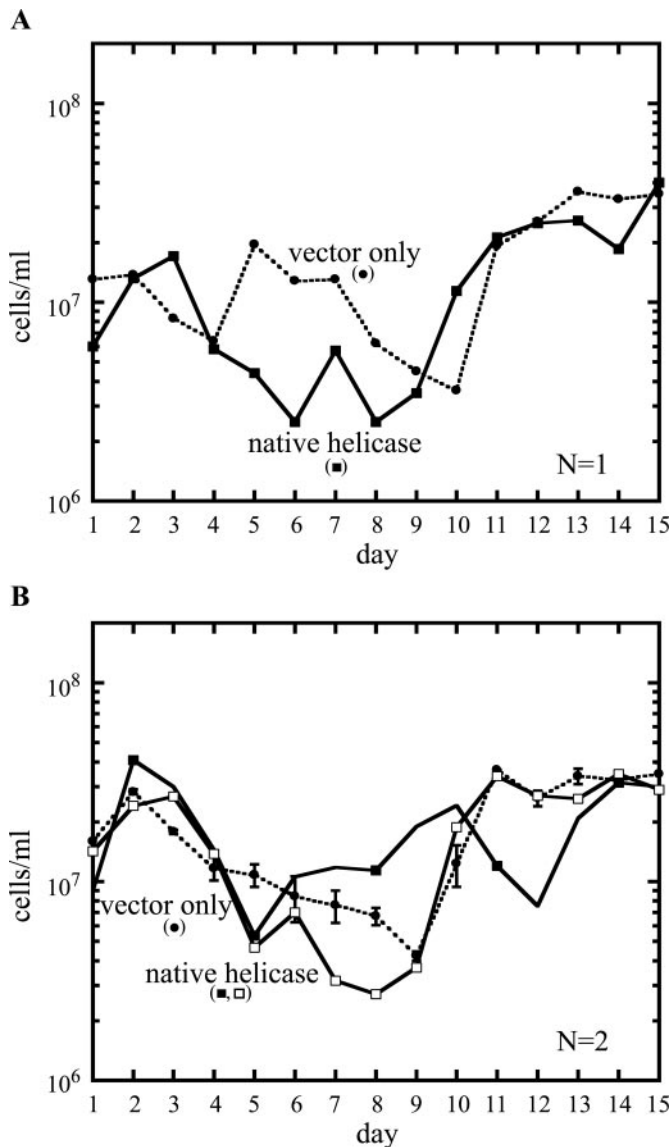
FIG. 6. **Native helicase overexpression in *trt1*⁻ cells.** *A,* as in Fig. 5, except *trt1*⁻ cells were used in 10-ml cultures. Cell density is shown for cells with either vector only (*broken line,* ●) or vector with the native helicase sequence (*solid line,* ■). A single growth curve (*n* = 1) was conducted for each strain. *B,* as in *A,* except two independent 100-ml cultures were maintained for each strain (*n* = 2). The two vector-only cultures behaved similarly, and their data were thus averaged, resulting in a single curve with *error bars* (*broken line,* ●). Strains overexpressing the native helicase are depicted by *solid lines* (■ and □).

genes (SPAC212.11 and SPBCPT2R1.08c), whose expression is normally up-regulated during crisis (28). Two independent experiments were performed using *trt1*⁻ cells transformed with either vector only or vector expressing the native helicase sequence. The first experiment included a single growth curve for each strain, whereas the second experiment included two growth curves for each strain.

Strikingly, in the first experiment passage through crisis (the time when telomeres are shortest, population doubling time is the longest, and cells are elongated (18)) occurred at least 2 days earlier in cells overexpressing the native helicase (day 6–8) than in the vector-only control (day 10) (Fig. 6*A*). In the second experiment the two growth curves with vector-only strains were similar enough that the two curves could be averaged (Fig. 6*B*). Although these control cultures experienced crisis on day 9, one of the two cultures with the strain overexpressing native helicase experienced a first round of senescence

on day 5 followed by a second round on day 12 (Fig. 6*B*). Although multiple rounds of senescence have been previously observed (18), the occurrence of the first round on day 5 was unusually early. A second culture with cells overexpressing the native helicase had a broad nadir and the lowest cell density on day 8 (Fig. 6*B*). Taken together, cells overexpressing the native helicase passed through crisis sooner than cells with vector only.

Two independent sets of experiments were also conducted comparing the effect of overexpressing the mutant form of the helicase in *trt1*⁻ cells progressing through crisis. As mentioned above, the wild-type copies of the helicase gene (SPAC212.11 and SPBCPT2R1.08c) were still present in the genome and were expected to have their expression up-regulated during crisis (28). Therefore, overexpressed mutant helicase might function as a dominant negative and compete with the wild-type helicase for substrate. In the first experiment cells overexpressing the mutant helicase had lower growth rates than vector-only control cells even at early days in the growth curve before cells became sick from short telomeres (arrow 1 in Fig. 7, *A* and *B*). Such poor growth is consistent with the ragged colonies seen in the diploid cells overexpressing mutant helicase mentioned above. This decreased cell density relative to the vector-only control cells persisted throughout the entire growth curve. In addition, cells overexpressing the mutant helicase recovered from crisis about 1–2 days later than vector-only control cells (*arrow 2* in Fig. 7, *A* and *B*).

Cells were also collected daily for telomere analysis by Southern blot in the experiments shown in Figs. 6*B* and 7*B*. Survivors had linear chromosomes, telomeres were at their shortest when cells passed through crisis, and cells overexpressing helicase did not display evidence of altered recombination activity with respect to controls (data not shown). Therefore, despite the pronounced differences in cell behavior between strains, telomere dynamics appeared consistent between control strains and those overexpressing helicase.

Cells bearing the plasmid were also passaged through crisis by repeated re-streaking on plates, a procedure that consistently yields colonies only with circular chromosomes (18, 28). To test whether the presence of overexpressed native or mutant helicase would alter the chromosome structures of *trt1*⁻ survivors picked from plates, five colonies overexpressing the native helicase and four colonies overexpressing the mutant helicase were screened by Southern blot for telomere structure. All colonies screened had circular chromosomes (data not shown). Although the sample size was small, these results suggest no increased propensity to maintain linear chromosomes in the presence of either overexpressed helicase form.

DISCUSSION

The results presented here demonstrate that two telomere-proximal *S. pombe* genes (SPAC212.11 and SPBCPT2R1.08c) are homologous to the RecQ helicase family. Conservation of residues exists throughout the seven canonical consensus regions (3) between SPAC212.11 and established members of the RecQ helicase family such as Sgs1 and Rqh1, and WRN and BLM, the causes of human Werner's syndrome and Bloom's syndrome, respectively. In most cases, conserved residues are identical between the proteins, such as in the critical Walker A-box, required for binding and hydrolysis of ATP, and Walker B-box, required for Mg²⁺ binding and ATP hydrolysis (43), although many residues are similar. Although SPAC212.11 is evolutionarily similar to all of the helicases to which it was compared, it has the most similarity to human WRN. Nevertheless, the possibility remains that SPAC212.11 is a member of a different helicase family or that it is not even a functional helicase. Other proteins with DNA-dependent ATPase activity
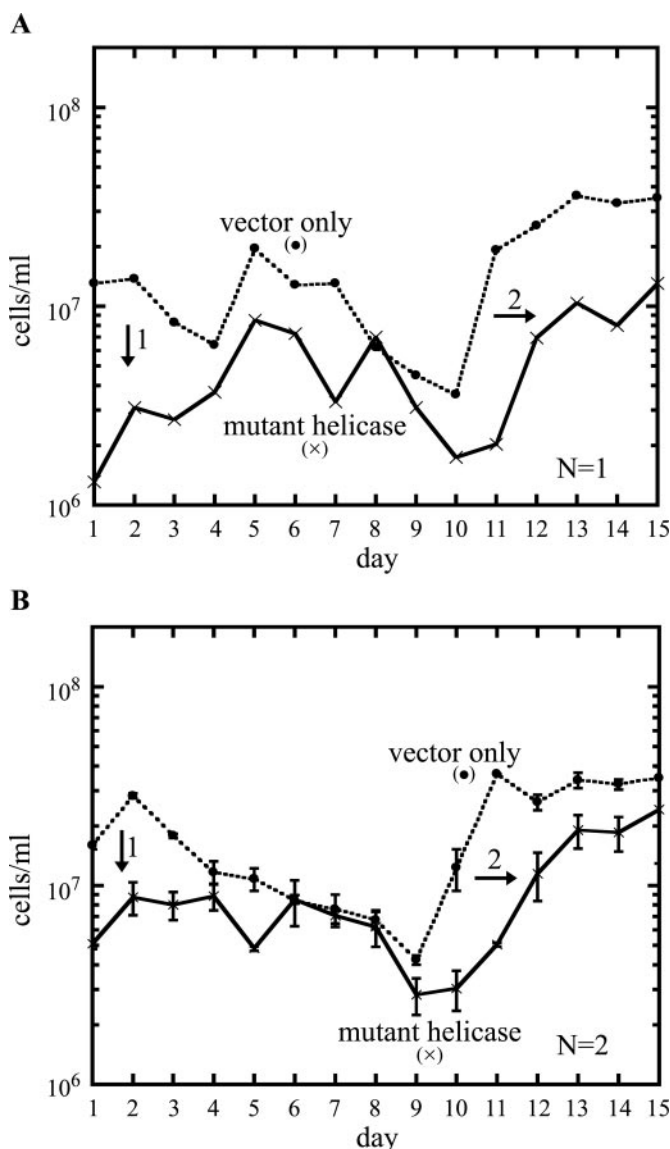
A

B

Fig. 7. **Mutant helicase overexpression in *trt1⁻* cells.** *A*, as in Fig. 5, except *trt1⁻* cells were used in 10-ml cultures. Cell density is shown for cells with either vector only (*broken line*, ●) or vector with the mutant helicase sequence (*solid line*, ×). A single growth curve (*n* = 1) was conducted for each strain. *Arrows* are explained in "Results." *B*, as in *A*, except two independent 100-ml cultures were maintained for each strain (*n* = 2). Replicates behaved similarly, and thus, their data were averaged and displayed with *error bars*. Vector-only cells are represented by the *broken line* (●), and cells overexpressing the mutant helicase are represented by the *solid line* (×).

and homology to helicases lack helicase activity, such as budding yeast Rad26 (human homolog Cockayne syndrome B protein) (51, 52).

Strikingly, cells overexpressing a cloned domain of SPAC212.11 that encompasses the region with predicted helicase activity entered into and exited from crisis earlier than cells bearing empty vector (Fig. 6), whereas cells overexpressing a protein designed to be catalytically dead had delayed exit from crisis (Fig. 7). The catalytically dead protein had two amino acid changes (in the Walker A-box and Walker B-box motifs) that are expected to destroy the activity of a RecQ helicase. Thus, these results provide strong support for the hypothesis that SPAC212.11 encodes an ATPase that facilitates progression through crisis. Additional biochemical studies are required to test for ATP-dependent catalysis of DNA unwinding. It should be noted that since wild-type protein from

the genomic copies of SPAC212.11 and SPBCPT2R1.08c was presumably expressed during recovery from crisis (28) and the wild-type protein may have higher affinity for substrate than the cloned form, it is possible that the effects observed here were less pronounced than would have been seen in a null background.

Mechanisms by which RecQ helicases might function in telomere maintenance were recently detailed (4, 11, 53). These non-mutually exclusive roles include resolving G-quadruplexes possibly at telomeres (9) that may interfere with recombination (5), aiding recombination at telomeres (54) and dissociating toxic telomeric D loop intermediates that damaged telomeres may form (10, 11, 23). Thus, RecQ helicases may promote beneficial recombination while suppressing promiscuous recombination (2).

The findings here, although completely consistent with the above hypotheses, are also supportive of a scenario in which the substrate(s) of SPAC212.11 includes abnormal telomeres, since the helicase is significantly expressed only in cells experiencing crisis (28) and appears to have no effect in wild-type cells (Fig. 5 and data not shown). Consistent with this, BLM and WRN localize to telomeric foci exclusively in ALT cells (11, 19). Interestingly, cells bearing vector-only or those overexpressing the catalytically dead protein form behaved very reproducibly (Fig. 7), whereas those overexpressing the active helicase form displayed more erratic behavior (Fig. 6). These fluctuations suggest that SPAC212.11 may promote a stochastic activity, such as recombination, that is apparently beneficial for recovering from crisis.

Lower eukaryotic species such as yeast generally contain only a single RecQ family representative (1). Because higher organisms usually have multiple family members, it does not seem unreasonable that *S. pombe* might have a second RecQ family member in addition to Rqh1, the previously identified fission yeast RecQ helicase. Any helicase activity from SPAC212.11 may act instead of, or with Rqh1.

There have been several reports of helicase genes at fungal chromosome ends. In *Saccharomyces cerevisiae*, the sub-telomeric Y′ elements are 5–6-kb tandem repeats that encode a DNA helicase, Yrf1, that is amplified in telomerase-negative cells (55). Two other distantly related fungi, *Magnaporthe grisea* and *Ustilago maydis*, have putative RecQ helicases at their telomeres (56, 57). These multiple examples of helicases located at telomeres suggest that telomeric helicases might date back to the early stages of fungal evolution and may be an adaptive response to life without telomerase (56).

REFERENCES

1. Bachrati, C. Z., and Hickson, I. D. (2003) *Biochem. J.* **374,** 577–606
2. Wu, L., and Hickson, I. D. (2002) *Mutat. Res.* **509,** 35–47
3. Gorbalenya, A. E., Koonin, E. V., Donchenko, A. P., and Blinov, V. M. (1989) *Nucleic Acids Res.* **17,** 4713–4730
4. Hickson, I. D. (2003) *Nat. Rev. Cancer* **3,** 169–178
5. Mohaghegh, P., Karow, J. K., Brosh Jr., R. M., Jr., Bohr, V. A., and Hickson, I. D. (2001) *Nucleic Acids Res.* **29,** 2843–2849
6. Li, J. L., Harrison, R. J., Reszka, A. P., Brosh, R. M., Jr., Bohr, V. A., Neidle, S., and Hickson, I. D. (2001) *Biochemistry* **40,** 15194–15202
7. Cech, T. R. (2000) *Angew. Chem. Int. Ed. Engl.* **39,** 34–43
8. Williamson, J. R., Raghuraman, M. K., and Cech, T. R. (1989) *Cell* **59,** 871–880
9. Schaffitzel, C., Berger, I., Postberg, J., Hanes, J., Lipps, H. J., and Pluckthun, A. (2001) *Proc. Natl. Acad. Sci. U. S. A.* **98,** 8572–8577
10. Griffith, J. D., Comeau, L., Rosenfield, S., Stansel, R. M., Bianchi, A., Moss, H., and de Lange, T. (1999) *Cell* **97,** 503–514
11. Opresko, P. L., Otterlei, M., Graakjaer, J., Bruheim, P., Dawut, L., Kolvraa, S., May, A., Seidman, M. M., and Bohr, V. A. (2004) *Mol. Cell* **14,** 763–774
12. Tham, W. H., and Zakian, V. A. (2002) *Oncogene* **21,** 512–521
13. Greider, C. W. (1996) *Annu. Rev. Biochem.* **65,** 337–365
14. McEachern, M. J., Krauskopf, A., and Blackburn, E. H. (2000) *Annu. Rev. Genet.* **34,** 331–358
15. Bryan, T. M., Englezou, A., Gupta, J., Bacchetti, S., and Reddel, R. R. (1995) *EMBO J.* **14,** 4240–4248
16. Reddel, R. R. (2003) *Cancer Lett.* **194,** 155–162

17. Lundblad, V., and Blackburn, E. H. (1993) *Cell* **73,** 347–360
18. Nakamura, T. M., Cooper, J. P., and Cech, T. R. (1998) *Science* **282,** 493–496
19. Stavropoulos, D. J., Bradshaw, P. S., Li, X., Pasic, I., Truong, K., Ikura, M., Ungrin, M., and Meyn, M. S. (2002) *Hum. Mol. Genet.* **11,** 3135–3144
20. Broccoli, D., Smogorzewska, A., Chong, L., and de Lange, T. (1997) *Nat. Genet.* **17,** 231–235
21. Opresko, P. L., von Kobbe, C., Laine, J. P., Harrigan, J., Hickson, I. D., and Bohr, V. A. (2002) *J. Biol. Chem.* **277,** 41110–41119
22. Machwe, A., Xiao, L., and Orren, D. K. (2004) *Oncogene* **23,** 149–156
23. Huang, P., Pryde, F. E., Lester, D., Maddison, R. L., Borts, R. H., Hickson, I. D., and Louis, E. J. (2001) *Curr. Biol.* **11,** 125–129
24. Johnson, F. B., Marciniak, R. A., McVey, M., Stewart, S. A., Hahn, W. C., and Guarente, L. (2001) *EMBO J.* **20,** 905–913
25. Cohen, H., and Sinclair, D. A. (2001) *Proc. Natl. Acad. Sci. U. S. A.* **98,** 3174–3179
26. Schulz, V. P., Zakian, V. A., Ogburn, C. E., McKay, J., Jarzebowicz, A. A., Edland, S. D., and Martin, G. M. (1996) *Hum. Genet.* **97,** 750–754
27. Wyllie, F. S., Jones, C. J., Skinner, J. W., Haughton, M. F., Wallis, C., Wynford-Thomas, D., Faragher, R. G., and Kipling, D. (2000) *Nat. Genet.* **24,** 16–17
28. Mandell, J. G., Bähler, J., Volpe, T. A., Martienssen, R. A., and Cech, T. R. (2005) *Genome Biol.* **6,** RI.1–RI.15
29. Maundrell, K., Hutchison, A., and Shall, S. (1988) *EMBO J.* **7,** 2203–2209
30. Mertins, P., and Gallwitz, D. (1987) *Nucleic Acids Res.* **15,** 7369–7379
31. Brizzard, B. L., Chubet, R. G., and Vizard, D. L. (1994) *Biotechniques* **16,** 730–735
32. McLeod, M., Stein, M., and Beach, D. (1987) *EMBO J.* **6,** 729–736
33. Broker, M., and Bauml, O. (1989) *FEBS Lett.* **248,** 105–110
34. Wach, A., Brachat, A., Pohlmann, R., and Philippsen, P. (1994) *Yeast* **10,** 1793–1808
35. Haering, C. H., Nakamura, T. M., Baumann, P., and Cech, T. R. (2000) *Proc. Natl. Acad. Sci. U. S. A.* **97,** 6367–6372
36. Alfa, C., Fantes, P., Hyams, J., McLeod, M., and Warbrick, E. (1993) *Experiments with Fission Yeast*, pp. 95–98, Cold Spring Harbor Laboratory Press, Cold Spring Harbor, NY
37. Thompson, J. D., Higgins, D. G., and Gibson, T. J. (1994) *Nucleic Acids Res.* **22,** 4673–4680
38. Bandyopadhyay, A., Matsumoto, T., and Maitra, U. (2000) *Mol. Biol. Cell* **11,** 4005–4018
39. Baumann, P., and Cech, T. R. (2000) *Mol. Biol. Cell* **11,** 3265–3275
40. Brown, T. (1993) *Current Protocols in Molecular Biology*, pp. 4.9.1–4.9.14, John Wiley & Sons, Inc., New York
41. Church, G. M., and Gilbert, W. (1984) *Proc. Natl. Acad. Sci. U. S. A.* **81,** 1991–1995
42. Tatusov, R. L., Natale, D. A., Garkavtsev, I. V., Tatusova, T. A., Shankavaram, U. T., Rao, B. S., Kiryutin, B., Galperin, M. Y., Fedorova, N. D., and Koonin, E. V. (2001) *Nucleic Acids Res.* **29,** 22–28
43. Walker, J. E., Saraste, M., Runswick, M. J., and Gay, N. J. (1982) *EMBO J.* **1,** 945–951
44. Yu, C. E., Oshima, J., Fu, Y. H., Wijsman, E. M., Hisama, F., Alisch, R., Matthews, S., Nakura, J., Miki, T., Ouais, S., Martin, G. M., Mulligan, J., and Schellenberg, G. D. (1996) *Science* **272,** 258–262
45. Wood, V., Gwilliam, R., Rajandream, M. A., Lyne, M., Lyne, R., *et al.* (2002) *Nature* **415,** 871–880
46. Nakaseko, Y., Kinoshita, N., and Yanagida, M. (1987) *Nucleic Acids Res.* **15,** 4705–4715
47. Caruthers, J. M., and McKay, D. B. (2002) *Curr. Opin. Struct. Biol.* **12,** 123–133
48. Wang, L., Ogburn, C. E., Ware, C. B., Ladiges, W. C., Youssoufian, H., Martin, G. M., and Oshima, J. (2000) *Genetics* **154,** 357–362
49. Forsburg, S. L. (1993) *Nucleic Acids Res.* **21,** 2955–2956
50. Maundrell, K. (1990) *J. Biol. Chem.* **265,** 10857–10864
51. van Gool, A. J., Verhage, R., Swagemakers, S. M., van de Putte, P., Brouwer, J., Troelstra, C., Bootsma, D., and Hoeijmakers, J. H. (1994) *EMBO J.* **13,** 5361–5369
52. Gray, M. D., Shen, J. C., Kamath-Loeb, A. S., Blank, A., Sopher, B. L., Martin, G. M., Oshima, J., and Loeb, L. A. (1997) *Nat. Genet.* **17,** 100–103
53. Du, X., Shen, J., Kugan, N., Furth, E. E., Lombard, D. B., Cheung, C., Pak, S., Luo, G., Pignolo, R. J., DePinho, R. A., Guarente, L., and Johnson, F. B. (2004) *Mol. Cell. Biol.* **24,** 8437–8446
54. Tarsounas, M., Munoz, P., Claas, A., Smiraldo, P. G., Pittman, D. L., Blasco, M. A., and West, S. C. (2004) *Cell* **117,** 337–347
55. Yamada, M., Hayatsu, N., Matsuura, A., and Ishikawa, F. (1998) *J. Biol. Chem.* **273,** 33360–33366
56. Gao, W., Khang, C. H., Park, S. Y., Lee, Y. H., and Kang, S. (2002) *Genetics* **162,** 103–112
57. Sanchez-Alonso, P., and Guzman, P. (1998) *Genetics* **148,** 1043–1054
58. Ellis, N. A., Groden, J., Ye, T. Z., Straughen, J., Lennon, D. J., Ciocci, S., Proytcheva, M., and German, J. (1995) *Cell* **83,** 655–666
59. Murray, J. M., Lindsay, H. D., Munday, C. A., and Carr, A. M. (1997) *Mol. Cell. Biol.* **17,** 6868–6875
60. Watt, P. M., Louis, E. J., Borts, R. H., and Hickson, I. D. (1995) *Cell* **81,** 253–260
61. Saitou, N., and Nei, M. (1987) *Mol. Biol. Evol.* **4,** 406–425
62. Fan, J. B., Chikashige, Y., Smith, C. L., Niwa, O., Yanagida, M., and Cantor, C. R. (1989) *Nucleic Acids Res.* **17,** 2801–2818